THE JOURNAL OF BIOLOGICAL CHEMISTRY
Vol. 280, No. 19, Issue of May 13, pp. 18797–18802, 2005
Printed in U.S.A.

Role of T-loop Phosphorylation in PDK1 Activation, Stability, and Substrate Binding*

Received for publication, January 26, 2005
Published, JBC Papers in Press, March 1, 2005, DOI 10.1074/jbc.M500977200

David Komander‡§¶, Gursant Kular§, Maria Deak§, Dario R. Alessi§, and Daan M. F. van Aalten‡‖

From the ‡Division of Biological Chemistry and Molecular Microbiology and the §MRC Protein Phosphorylation Unit, MSI/WTB Complex, School of Life Sciences, University of Dundee, Dundee DD1 5EH, Scotland

3-Phosphoinositide-dependent protein kinase-1 (PDK1) phosphorylates the T-loop of several AGC (cAMP-dependent, cGMP-dependent, protein kinase C) family protein kinases, resulting in their activation. Previous structural studies have revealed that the αC-helix, located in the small lobe of the kinase domain of PDK1, is a key regulatory element, as it links a substrate interacting site termed the hydrophobic motif (HM) pocket with the phosphorylated Ser-241 in the T-loop. In this study we have demonstrated by mutational analysis that interactions between the phosphorylated Ser-241 and the αC-helix are not required for PDK1 activity or substrate binding through the HM-pocket but are necessary for PDK1 to be activated or stabilized by a peptide that binds to this site. The structure of an inactive T-loop mutant of PDK1, in which Ser-241 is changed to Ala, was also determined. This structure, together with surface plasmon resonance binding studies, demonstrates that the PDK1(S241A)-inactive mutant possesses an intact HM-pocket as well as an ordered αC-helix. These findings reveal that the integrity of the αC-helix and HM-pocket in PDK1 is not regulated by T-loop phosphorylation.

3-Phosphoinositide-dependent protein kinase-1 (PDK1)[1] is a Ser/Thr protein kinase that activates at least 23 protein kinases belonging to the AGC (cAMP-dependent, cGMP-dependent, protein kinase C) family of protein kinases by phosphorylating their T-loops (1). PDK1 possesses an N-terminal catalytic domain and a C-terminal Pleckstrin Homology (PH) domain (2, 3). The latter binds with high affinity to the PtdIns(3,4,5)P_3 and PtdIns(3,4)P_2 second messengers that are generated by phosphatidylinositol 3-kinase following stimulation of cells with growth factors (3, 4). The recent determination of the structure of the PDK1 PH domain has revealed the molecular basis for its interaction with phosphoinositides (5). The only PDK1 AGC kinase substrates to also possess a PtdIns(3,4,5)P_3/PtdIns(3,4)P_2 binding PH domain are isoforms of PKB (also known as Akt) (1). Much evidence indicates that the mutual binding of PKB and PDK1 to PtdIns(3,4,5)P_3/PtdIns(3,4)P_2 at the plasma membrane co-localizes these enzymes and is necessary for PKB to be activated by PDK1 (6, 7). In contrast, the other PDK1 AGC kinase substrates, including p70 ribosomal S6-kinase (8), serum- and glucocorticoid-responsive kinase (9), and p90 ribosomal S6 kinase (10), do not bind PtdIns(3,4,5)P_3/PtdIns(3,4)P_2 or possess PH domains. Instead, these kinases possess conserved PDK1 docking sites located in a C-terminal region known as the hydrophobic motif (HM). Growth factors and hormones lead to the phosphorylation of the hydrophobic motif of these AGC kinases, significantly enhancing their ability to interact with PDK1 (4, 11, 12). The region on PDK1 that interacts with the hydrophobic motif of its substrates is termed the HM-pocket and is located on the N-terminal smaller lobe of the catalytic domain (13, 14). The structure of the PDK1 catalytic domain revealed that the HM-pocket consisted of a hydrophobic pocket adjacent to a positively charged phosphate binding pocket (15).

PDK1 itself is also an AGC kinase member and, like its substrates, requires to be phosphorylated at its T-loop (Ser-241) to be activated (16). *In vivo*, PDK1 is capable of autophosphorylation at Ser-241 by an intermolecular reaction and is thus constitutively phosphorylated at Ser-241 (17). The structural analysis of the PDK1 kinase domain has revealed that, similar to what has been observed in other kinases, the phosphorylated Ser-241 residue forms key interactions coordinating and aligning important catalytic motifs such as the αC-helix of the N-terminal lobe. The αC-helix plays a key role in all kinases as it contributes crucial residues to coordinating ATP. In PDK1 it positions the conserved Glu-130 residue such that it coordinates the conserved Lys-111, which interacts with the α-phosphate of ATP. This hydrogen bonding network is conserved in most protein kinases and is required for phosphoryl transfer. Many kinases are regulated by controlling the position and/or formation of the αC-helix. For example, the binding of cyclins to cyclin-dependent kinases (CDKs) induces a rotation of the αC-helix, leading to CDK activation (18–20). More recently the structure of PKBβ in the unphosphorylated, inactive state was reported to possess a completely disordered αC-helix (21). PDK1-mediated phosphorylation of PKBβ and interaction of PKBβ with its own hydrophobic motif (HM) led to

* This work was supported in part by the Association for International Cancer Research (to D. R. A.), Diabetes UK (to D. R. A. and D. M. F. v. A.) the Medical Research Council (to D. R. A.), the Moffat Charitable Trust (to D. R. A.), and the pharmaceutical companies supporting the Division of Signal Transduction Therapy Unit (AstraZeneca, Boehringer-Ingelheim, GlaxoSmithKline, Merck & Co. Inc., Merck KgaA, and Pfizer). The costs of publication of this article were defrayed in part by the payment of page charges. This article must therefore be hereby marked "*advertisement*" in accordance with 18 U.S.C. Section 1734 solely to indicate this fact.

The atomic coordinates and structure factors (code 2BIY) have been deposited in the Protein Data Bank, Research Collaboratory for Structural Bioinformatics, Rutgers University, New Brunswick, NJ (http://www.rcsb.org/).

¶ Supported by a Medical Research Council predoctoral fellowship. To whom correspondence may be addressed: Section of Structural Biology, Inst. of Cancer Research, Chester Beatty Laboratories, 237 Fulham Rd., London, SW3 6JB, UK. E-mail: david.komander@icr.ac.uk.

‖ Supported by a Wellcome Trust Senior Research fellowship and the EMBO Young Investigator Program. To whom correspondence may be addressed. E-mail: dava@davapc1.bioch.dundee.ac.uk.

[1] The abbreviations used are: PDK1, 3-phosphoinositide-dependent protein kinase-1; AGC, cAMP-dependent, cGMP-dependent, protein kinase C; HM, hydrophobic motif; PKB, protein kinase B; PKA, cAMP-dependent protein kinase; GST, glutathione *S*-transferase; HM-PRK2, hydrophobic motif peptide derived from PKC-related kinase-2.

ordering of this helix, resulting in PKB activation (22). This suggested a new regulatory αC-helix-dependent mechanism in PKB and posed the question of whether other AGC family members would be regulated in a similar manner. In PDK1, phosphorylated Ser-241 interacts with 2 residues on the αC-helix (Tyr-126 and Arg-129) (15), whereas PKBβ and PKA only possess a single interaction between the T-loop and the αC-helix (22, 23). Interestingly, the αC-helix also contributes hydrophobic as well as phosphate binding residues to the HM-pocket (Fig. 1*A*) (15). Likewise, in active PKBβ the formation of the αC-helix leads to the creation of a pocket resembling the HM-pocket of PDK1. This pocket binds intramolecularly to the phosphorylated hydrophobic motif of PKBβ, and this interaction is required for maximal activation. Similarly, occupancy of the HM-pocket of PDK1 with peptides encompassing the phosphorylated HM docking residues of its substrates activates PDK1 4–6-fold and also stabilizes the enzyme (13, 24). These observations have been interpreted as implying that PDK1 is activated through interaction with its substrates. In this study we explored the role of T-loop phosphorylation of PDK1 in regulating enzyme structure, activity, stability, and interaction with substrates.

MATERIALS AND METHODS

Protein Expression, Purification, and Crystallization—PDK1(S241A) (residues 51–359) was purified from baculovirus-infected Sf-21 cells as described previously for the 51–359 wild type PDK1 catalytic domain (15). For crystallization experiments, 50 μl of PDK1(S241A) at 6.8 mg/ml were mixed with 5 μl of ATP and incubated on ice for 1 h. The protein crystallized at 20 °C by mixing 1 μl of protein solution with 1 μl of mother liquor (2.2 M ammonium sulfate, 0.1 M Tris, pH 7.5). Prior to data collection, the crystals were soaked in mother liquor containing 15% glycerol.

Data Collection and Structure Determination—Diffraction data on the PDK1(S241A)·ATP complex were collected at the European Synchrotron Radiation Facility beamline ID14-EH1 (Grenoble, France) to 1.95 Å. The protein crystallized in the same space group ($P3_221$) with similar unit cell dimensions compared with the wild type PDK1·ATP complex structure (Protein Data Bank accession number 1h1w) (15) (Table I). The data were processed and scaled with the HKL suite (25), and the structure was solved by rigid body refinement using CNS (26) with the PDK1·ATP complex as a search model, followed by simulated annealing in CNS. Subsequent alternating rounds of refinement (in CNS and REFMACS 5) (27) and model building (in O) (28) were performed. Water and glycerol molecules as well as sulfate ions were included in final rounds of refinement, as was one molecule of ATP, respectively. ATP topologies were generated with PRODRG (29). Final statistics can be found in Table I.

Mutagenesis and Activity Assays—Mutants of PDK1 were generated using site-directed mutagenesis with the QuikChange mutagenesis kit (Stratagene) in the pEBG2T vector. PDK1 and the indicated mutants were expressed as glutathione *S*-transferase (GST) fusion protein in human embryonic kidney 293 cells and purified as described previously (13). PDK1 and mutants were assayed against the T308tide substrate peptide (KTFCGTPEYLAPEVRR) (13) in the absence or presence of 1 or 10 μM HM-PRK2 (REPRILSEEEQEMFRDFDYIADWC) (30) for 10 min at 30 °C in a 50-μl assay mixture in 50 mM Tris (pH 7.5), 0.1 mM EGTA, 0.1% 2-mercaptoethanol containing 1 mM substrate peptide, 10 mM magnesium acetate, 100 μM [γ-^{32}P] ATP (200 cpm/mol) as described previously (15). For the thermal stability experiments shown in Fig. 2, prior to assay 150 ng of wild type GST·PDK1 or indicated mutant GST·PDK1 in the presence or absence of 100 μM HM-PRK2 in a volume of 25 μl was placed in a 96-well PCR plate. Following incubation for 2 min on a 40–60 °C step temperature gradient in a PCR machine (MJ Research PTC-200 Gradient Cycler), PDK1 activity was assayed as described above employing T308tide.

Surface Plasmon Resonance Spectroscopy—Binding was analyzed in a BiaCore 3000 system (BiaCore AB, Stevenage, UK) according to Ref. 13. The biotinylated 24-residue peptide HM-PRK2 (Biotin-C12- REPRILSEEEQEMFRDFDYIADWC) was bound to a streptavidin-coated sensor chip (SA) (25 response units). 30 μl of the indicated concentration of wild type or mutant GST·PDK1 were injected at a flow rate of 30 μl/min in buffer HBS-P (10 mM HEPES, pH 7.4, 0.15 M NaCl, 0.005% (v/v) polysorbate-20) supplemented with 1 mM dithiothreitol. Specific interactions between HM-PRK2 and PDK1 proteins were obtained between the concentration range of 2.5–2000 nM PDK1. Steady state binding was determined at each concentration. Dissociation of PDK1 from the HM-PRK2 was monitored over a 1-min period. Regeneration of the sensor chip surface was performed with 10-μl injections of 0.05% SDS. The K_d of interaction was calculated as described previously (13) by fitting the data to a sigmoid curve using GraphPad Prism software.

TABLE I
Data collection and refinement statistics

Values between parentheses are for the highest resolution shell. All measured data were included in structure refinement.

	PDK(S241A) (51–359)·ATP complex
Beamline	ID14-EH1
Wavelength (Å)	0.933
Space group	$P3_221$
Unit cell (Å)	$a, b = 121.83$ $c = 47.75$
Resolution (Å)	25.0–1.95 (2.02–1.95)
Observed reflections	123183
Unique reflections	28782
Redundancy	4.3 (3.0)
Completeness (%)	90.5 (99.2)
R_{merge}	0.083 (0.416)
$I/\sigma I$	14.2 (2.3)
Reflections in test set	588
R_{cryst}	0.185
R_{free}	0.230
Protein residues	287
Water	166
Ligand atoms	31
SO_4^{2-} atoms	35
Glycerol atoms	42
Wilson B (Å^2)	24.2
⟨B⟩ protein (Å^2)	28.3
⟨B⟩ water (Å^2)	39.5
⟨B⟩ ligand (Å^2)	33.7
Bond length (Å)	0.014
Bond angles (°)	1.5
Main chain B (Å^2)	0.9

RESULTS AND DISCUSSION

Mutation of Residues on PDK1 That Interact with Phosphorylated Ser-241—The crystal structure of PDK1 (15) revealed that the phosphorylated Ser-241 makes hydrogen bond interactions to 4 residues, Arg-204 and Lys-228 from the C-terminal lobe and Tyr-126 and Arg-129 from the αC-helix in the N-terminal lobe. The highly conserved Arg-204 immediately precedes the catalytic Asp-205, and the presence of this RD motif places PDK1 in the group of RD kinases (31, 32). Arg-204 is directly connected to the catalytic machinery because of its position within the catalytic loop and controls the fold of the activation loop after interaction with the phosphorylated Ser-241. Lys-228 may also play a role in aligning catalytic site residues, such as the Mg^{2+} interacting residue Asp-223 in the DFG motif. This is similar to the suggested role of the corresponding residues Arg-165 and Lys-189 in PKA (33). Mutational analysis of the RD Arg in both Ser/Thr and Tyr protein kinases has confirmed its importance (34–36). Interestingly, the residue equivalent to PDK1 Arg-204 in PKBβ (Arg-274) was recently found to be mutated in a human family with severe diabetes and insulin resistance (37).

To assess the role of Arg-204 and Lys-228 in PDK1, these residues were mutated to Ala. The effect that this had on PDK1 catalytic activity was assessed with an assay employing a peptide substrate (T308tide). In addition, the ability of these mutants to be activated by a peptide encompassing the hydrophobic motif of the PKC-related kinase-2 (PRK2), termed HM-PRK2, was also measured. In these assays HM-PRK2 was utilized at 1 μM, which maximally activates wild type PDK1, and at 10 μM, so activation could be detected if the affinity of

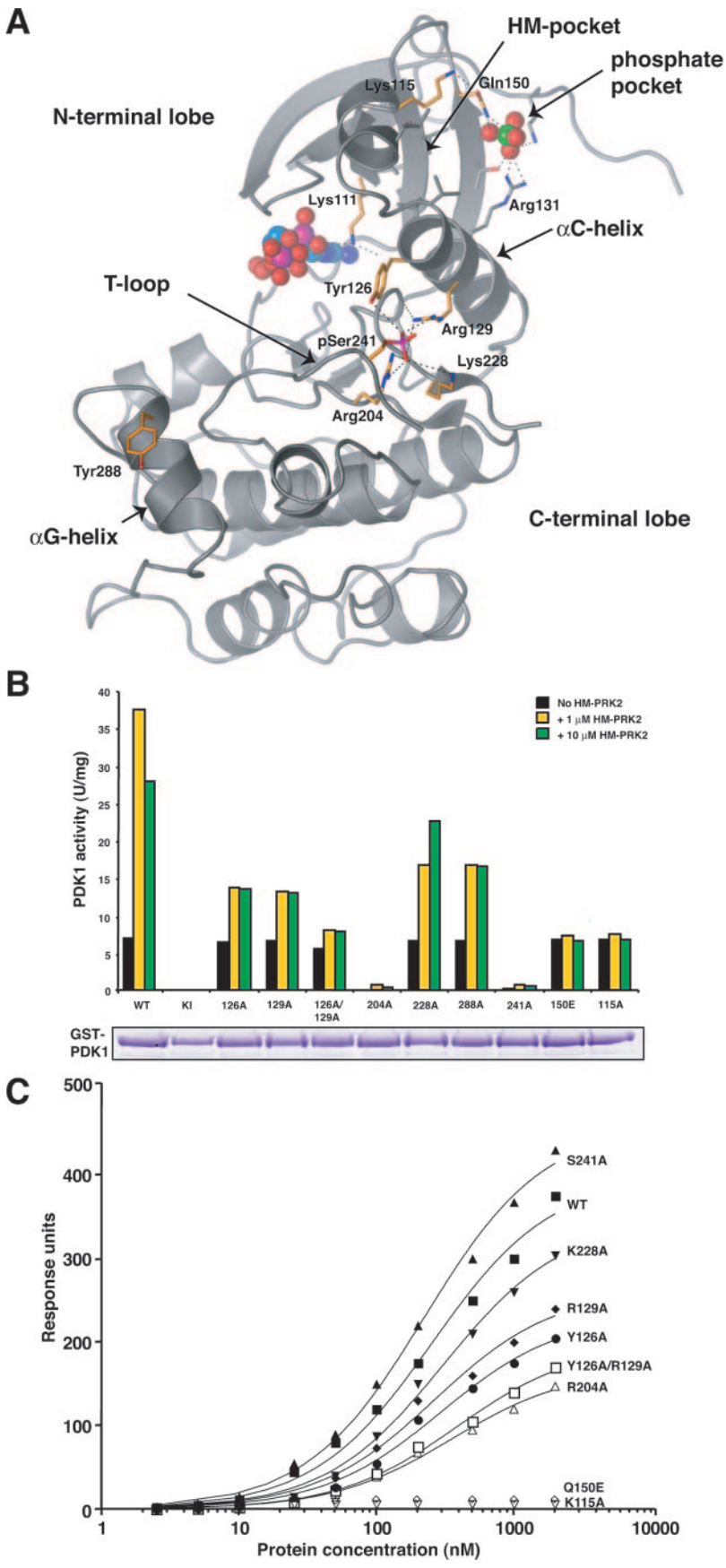

FIG. 1. **Analysis of residues coordinated by T-loop phosphorylation.** *A*, structure of the native PDK1 kinase domain (Protein Data Bank accession number 1h1w) (15) in schematic representation. Residues discussed under "Results" are drawn as a stick representation with *blue* nitrogen atoms, *red* oxygen atoms, and *purple* phosphorus atoms. Residues with *orange* carbon atoms have been mutated in this study, whereas residues with *gray* carbon atoms have been mutated in a previous analysis (15). The ATP molecule and the sulfate molecule present in the phosphate pocket are drawn as *colored spheres*, and hydrogen bonds are indicated as *black dotted lines*. *B*, activity measurements of wild type (*WT*) PDK1, kinase-dead (*KI*) PDK1, and indicated mutants of PDK1. Activity was measured in the absence of HM-PRK2 (*black*) or in the presence of 1 μM (*yellow*) or 10 μM (*green*) HM-PRK2 peptide. Equivalent amounts of wild type and mutant PDK1 were used as shown by a Coomassie-stained gel. *C*, binding of wild type or indicated mutants of GST·PDK1 to the HM-PRK2 peptide was analyzed by surface plasmon resonance BiaCore analysis as described under "Materials and Methods." Binding was analyzed over a range of PDK1 protein concentrations (2.5–2000 nM), and the response level at the steady state binding was plotted *versus* the log of the PDK1 concentration. For the mutants for which significant binding could be detected, estimated K_ds were obtained by fitting the response curves to the 1:1 Langmuir binding model using GraphPad Prism. The apparent K_ds were: wild type PDK1 = 72 ± 5 nM, PDK1(S241A) = 67 ± 4 nM, PDK1(K228A) = 270 ± 7 nM, PDK1(R129A) = 365 ± 5 nM, PDK1(Y126A) = 380 ± 3 nM, PDK1(Y126A,R129A) = 410 ± 8 nM, PDK1(R204A) = 478 ± 10 nM. For the PDK1(Q150E) and PDK1(K115A) mutants the binding was too weak to be able to quantitatively assess the K_d.

the PDK1 mutant for the peptide were reduced. The ability of wild type and PDK1 mutants to interact directly with biotinylated HM-PRK2 peptide was also assessed, using a quantitative surface plasmon resonance assay. As expected, the PDK1(R204A) mutant possessed negligible catalytic activity in the presence or absence of HM-PRK2, similar to that of a

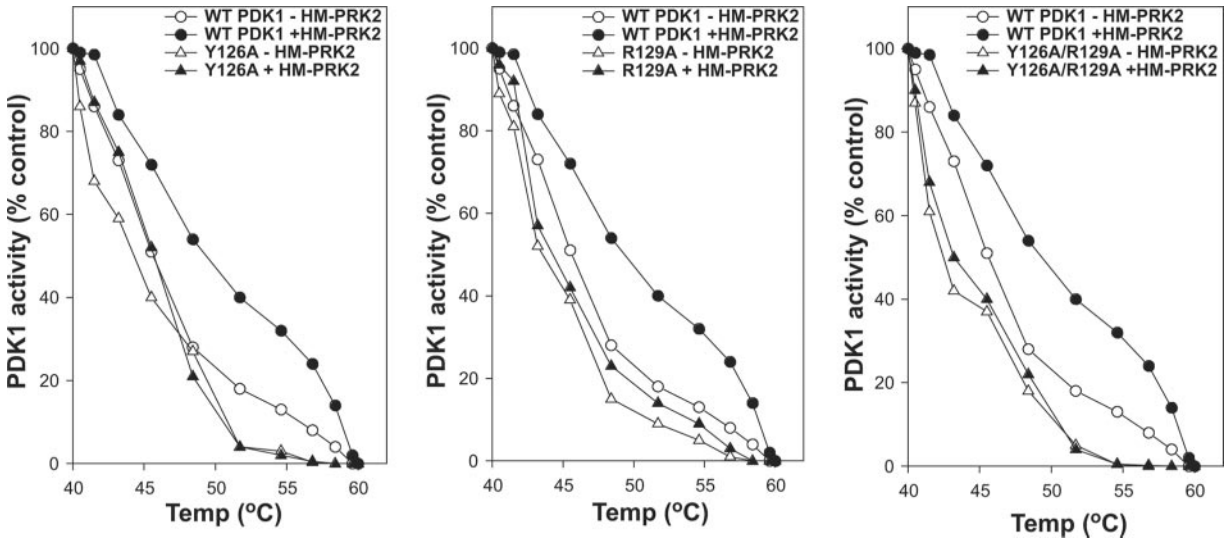

FIG. 2. **Stability analysis of PDK1 αC-helix mutants.** The wild type GST·PDK1 (*circles*) or the indicated mutants of GST·PDK1 (*triangles*) were incubated in the presence (*closed symbols*) or absence (*open symbols*) of 100 μM HM-PRK2. The samples were then incubated for 2 min at the indicated temperature prior to assay at 30 °C as described under "Materials and Methods." The activity of PDK1 obtained by incubation at 40 °C was taken as 100%. The data are presented as the average value of two separate experiments in which each condition was assayed in triplicate.

previously characterized catalytically inactive PDK1 mutant, PDK1(K111A) (Fig. 1*B*). However, the PDK1(R204A) mutant still interacted with HM-PRK2 (K_d 478 ± 10 nM), albeit with reduced affinity compared with wild type PDK1 (K_d 72 ± 5 nM) but with significantly greater affinity than two HM-pocket mutants of PDK1, PDK1(Q150E) and PDK1(K115A), that do not show detectable binding to HM-PRK2 (Fig. 1*C*). In contrast, PDK1(K228A) was normally active, could be further activated by 1 μM HM-PRK2, and bound HM-PRK2 in the surface plasmon resonance assay with high affinity (K_d 270 ± 7 nM). In PKA, mutation of the residue Lys-189 equivalent to PDK1 Lys-228 was similarly observed to have no effect on catalytic activity (38).

Next, Tyr-126 and Arg-129 were mutated either individually or together to Ala to disrupt the connection of phosphorylated Ser-241 with the αC-helix. In the absence of HM-PRK2, these PDK1 mutants possessed similar activity as wild type PDK1. However, the PDK1(Y126A) and PDK1(R129A) mutants were activated only 2-fold, at either 1 and 10 μM HM-PRK2, compared with 5-fold activation for wild type PDK1 (Fig. 1*B*). As similar activation was observed at both concentrations of HM-PRK2, this indicates that the affinity of these mutants for HM-PRK2 is similar to that of wild type PDK1 but the transmission of binding to the catalytic residues is impaired. Consistent with this notion, the double PDK1(Y126A,R129A) mutant was barely activated by HM-PRK2 (Fig. 1*B*). Interestingly, the PDK1(Y126A) (K_d 380 ± 3 nM), PDK1(R129A) (K_d 365 ± 5 nM), and PDK1(Y126A,R129A) (K_d 410 ± 8 nM) still interacted with significant affinity with HM-PRK2 (Fig. 1*C*). In PKA and PKBβ there is only a single interaction of the αC-helix with the phosphorylated T-loop, mediated by a His residue. Mutation of His-87 in the αC-helix of PKA that interacts with the phosphorylated Thr-197 at the T-loop impairs the catalytic activity of PKA (39), in contrast to what is observed for PDK1. To our knowledge the effect of mutating the equivalent residue on PKBβ (His-196) has not been investigated.

It has previously been shown, using thermal denaturation studies, that binding of HM-PRK2 to PDK1 also significantly thermostabilized PDK1 (13). We investigated whether the interaction of the αC-helix of PDK1 with the phosphorylated T-loop was required for HM-PRK2 to stabilize PDK1. Wild type PDK1 and mutant PDK1(Y126A), PDK1(R129A), and PDK1(Y126A,R129A) were incubated for 2 min at temperatures ranging from 40 to 60 °C prior to assay at 30 °C. Consistent with our previous work (13), wild type PDK1 was inactivated in temperature-dependent manner and was significantly stabilized in the presence of HM-PRK2 (Fig. 2). However, although the PDK1(Y126A), PDK1(R129A), and PDK1(Y126A,R129A) mutants showed similar stability to wild type PDK1 in the absence of HM-PRK2, they were not stabilized following the addition of HM-PRK2. These results indicate that the ability of HM-PRK2 to stabilize PDK1 through binding to the HM-pocket requires the interaction of the αC-helix with the phosphorylated T-loop.

Structure of the Inactive PDK1(S241A) Mutant Kinase Domain in Complex with ATP—The finding that the double PDK1(Y126A,R129A) mutant still interacted with HM-PRK2 (K_d 410 ± 8 nM) suggested that formation of the αC-helix of PDK1 was independent of Ser-241 phosphorylation. This notion was confirmed by the finding that the inactive PDK1(S241A) still interacted with HM-PRK2 with high affinity (K_d 67 ± 4 nM) (Fig. 1*C*). To investigate this further, the PDK1(S241A) mutant (residues 51–359) was crystallized in the presence of ATP without Mg^{2+} ions, employing similar conditions described for the wild type PDK1 kinase domain complexes. The structure was solved by molecular replacement using the previously determined PDK1 kinase domain structure (Protein Data Bank accession number 1h1w) (15). The overall structure of the PDK1(S241A) mutant is similar to the wild type PDK1·ATP complex (root mean square deviation 0.19 Å), with most of the larger deviations observed in the T-loop region introduced by the mutation (Fig. 3, *A* and *D*). One molecule of ATP is present at the nucleotide-binding site, which shows no structural deviations from the ATP molecule in the wild type PDK1·ATP complex (15) (maximum atomic shift 0.4 Å). In contrast to the wild type PDK1 kinase domain structure in which several T-loop residues (residues 233–236) were disordered, electron density for these residues is clearly defined in the PDK1(S241A) structure (Fig. 3*C*). The region of the T-loop surrounding Ser-241 (residues 230–245, *yellow* in Fig. 3, *C* and *D*) in the PDK1(S241A) structure adopts a markedly different conformation compared with wild type PDK1 (Fig. 3*D*). The Cβ carbon of Ala-241 is shifted by 10.1 Å compared with the Cβ carbon of Ser-241 in the wild type structure and is buried in a hydrophobic pocket lined by Leu-254, Val-249, Phe-291, and Leu-253 of the C-lobe. Moreover, the movement of

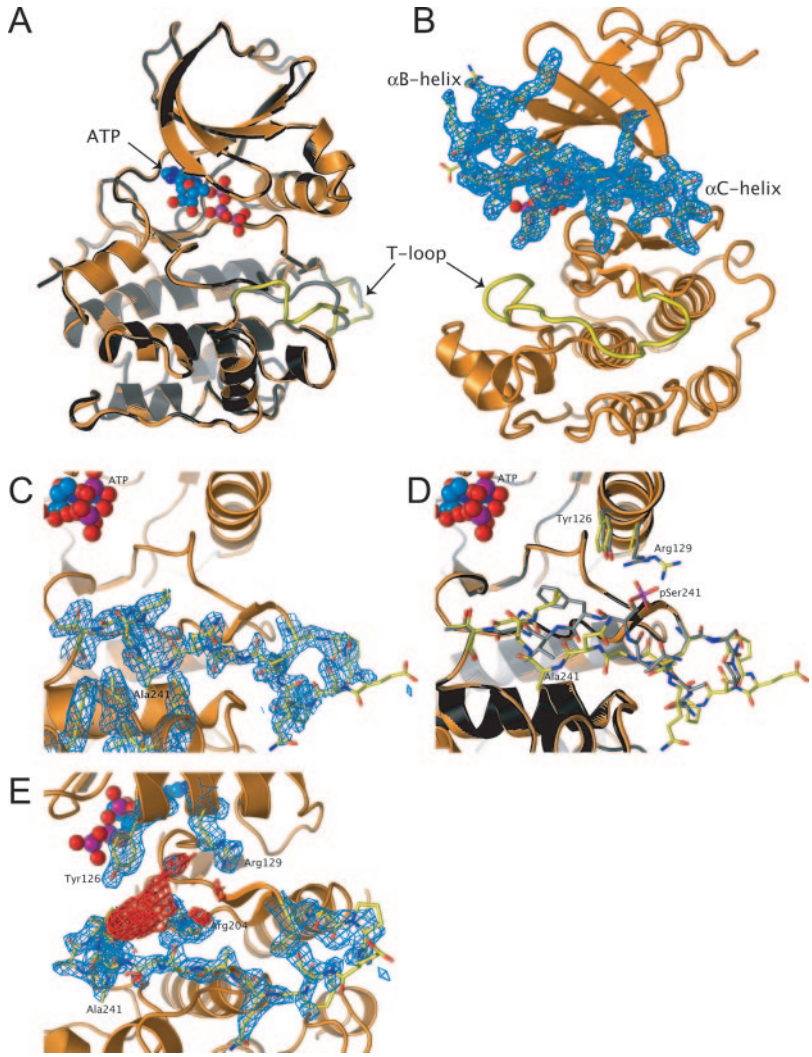

FIG. 3. **Structure of the PDK1(S241A) mutant.** *A*, overall structure of the PDK1(S241A)·ATP complex (*orange*) superimposed onto the PDK1·ATP complex (*black*). The ATP molecule is drawn in *sphere* representation. The only marked difference observed concerns the mutated T-loop (*yellow* and *gray*, respectively). *B*, in the PDK1(S241A) mutant structure, residues of the αC-helix are drawn in *stick* representation with *blue* nitrogen atoms, *red* oxygen atoms, and *yellow* carbon atoms. A $2F_o - F_c$ electron density map, contoured at 1 σ, is drawn in *blue* and displays well ordered density for all residues of the αB- and αC-helices and, therefore, an intact HM and phosphate pocket. *C*, a $2F_o - F_c$ electron density map (*blue*) contoured at 1 σ is drawn for the residues of the T-loop (coloring as in *panel B*). *D*, the T-loop position of PDK1(S241A) (*yellow*) deviates significantly from wild type PDK1 (*gray*). *E*, strong $F_o - F_c$ electron density, in red and contoured at 2.5 σ, is present at the site where the phosphate group was located in the wild type PDK1 structure, indicating a presumably negatively charged unidentified ligand. Residues Tyr-126, Arg-129, and Arg-204 are ordered in the structure, whereas Lys-228 lacks electron density.

Ser-241 in the PDK1(S241A) structure displaces Asn-240, Phe-242, and Val-243 by several Å compared with the wild type structure, resulting in a shift of the whole T-loop by a distance equivalent to 2 residues so that the carbonyl function of Arg-238 in the PDK1(S241A) structure takes the position of the carbonyl of Asn-240 in the wild type structure (located within 1.3 Å, Fig. 3*D*).

Consistent with the biochemical data, we find that the PDK1(S241A) structure displays fully ordered density for the αC-helix as well as the adjacent αB-helix (Fig. 3*B*, maximum atomic shift 0.4 Å). The PDK1(S241A) also displays a well ordered HM-pocket, indistinguishable from that of wild type PDK1. This shows that T-loop phosphorylation of PDK1 only has a role for enzyme activity and stability but not for formation of the αC-helix and, hence, docking to substrates via the HM-pocket. To date, no dephosphorylated T-loop structure of PKA has been solved, and the only other inactive AGC kinase crystallized apart from PKBβ is the N-terminal catalytic domain of MSK1 (40). This structure revealed an autoinhibited conformation in which a novel, three-stranded β-sheet occupies the position of the αC-helix in the N-terminal lobe, rendering the protein inactive (40). Recently, the phosphorylated, active structure of the catalytic domain of PKCθ AGC kinase was reported, which possesses similar features to that of PKA, PDK1, and activated PKBβ (41). In PKCθ, similar to PKBβ, the αC-helix creates an HM-pocket, which forms an intramolecular interaction with its own phosphorylated hydrophobic motif (41). A major difference, however, is that the phosphorylated T-loop in PKCθ does not interact with the αC-helix. The only charged interaction conserved in all PKC isoforms between the PKCθ αC-helix and the C-terminal lobe of the kinase domain is between Glu-528 (in the C-lobe), which interacts with Arg-430 (in αC-helix). As the phosphorylated T-loop in PKCθ does not interact with the αC-helix, PKCθ may be similar to PDK1 in that formation of the αC-helix is independent of T-loop phosphorylation.

Strikingly, in the PDK1(S241A) structure, strong electron density is observed at the site where the phosphate group is located in wild type PDK1 (Fig. 3*E*). The large, bulky electron density does not resemble any obvious component from the crystallization condition and was therefore not interpreted in the refinement procedure. The electron density is surrounded by residues Tyr-126, Arg-129, and Arg-204. Tyr-126 and Arg-204 adopt the same conformation as in wild type PDK1, whereas Arg-129 adopts a different conformation (Fig. 3*D*). The fourth residue interacting with the phosphorylated Ser-241 in the wild type structure, namely Lys-228, is disordered in the PDK1(S241A) structure. These observations suggest that a potentially negatively charged ligand occupied the unassigned density, possibly in the shape of a tetrahedral oxy-anion. A range of common oxy-anions (such as phosphate, sulfate, pyrophosphate) was included in the refinement procedure in an attempt to identify the ligand but without convincing results (data not shown). Interestingly, similar observations with negatively charged ligands in a positively charged pocket in a similar location have been made in a number of other crystal

structures of protein kinases such as glycogen synthase kinase 3β (42, 43), Chk1 (44), casein kinase 2 (CK2) (45), and phosphorylase kinase (PhK) (36). A common feature of these kinases with PDK1 is that they all belong to the RD class of protein kinases. The site of oxy-anion interaction has recently been named the RD-pocket, as the RD Arg (Arg-204 in PDK1) is a main contributor to the positively charged nature of the pocket (32). Phosphorylase kinase is not activated by phosphorylation in the T-loop but instead contains a negatively charged Glu residue that serves to align the catalytic machinery (36, 46). Interestingly, in the structure of a T-loop mutant of phosphorylase kinase in which the T-loop Glu residue was mutated to a Ser, a phosphate molecule occupies the site of the former negative charge contributed by the Glu residue, and no overall conformational changes are observed (36). This situation is similar to that observed in PDK1. From the current knowledge of how PDK1 is regulated it is not clear whether the ability of this site in unphosphorylated PDK1 to bind oxy-anions is physiologically important.

CONCLUSIONS

We have investigated how PDK1 T-loop phosphorylation affects activation and peptide binding in the HM-pocket. The biochemical and structural data show that T-loop phosphorylation of PDK1 is not required for the structural integrity of the αC-helix and the HM-pocket. Furthermore, the basal activity of PDK1 in the absence of the HM-PRK2 is not influenced by the interaction of the αC-helix with the phosphorylated T-loop residue. However, activation of PDK1 by HM-PRK2 is abolished in the PDK1(Y126A,R129A) mutant, which lacks contacts between the phosphorylated T-loop and the HM-pocket through the central αC-helix. Moreover, this mutant can no longer be stabilized to thermal denaturation in the presence of HM-PRK2. Thus it appears that these interactions enable the binding of PDK1 to the HM-motif of its substrates to be communicated to the catalytic residues. Interestingly, the three inactive structures of AGC kinases crystallized to date, namely PKBβ (21), MSK1 (40), and PDK1(S241A) (Fig. 3), display markedly different features, indicating that a variety of mechanisms exist to account for the activation of these enzymes by T-loop phosphorylation. In contrast, the active forms of the four AGC kinases crystallized to date, namely PDK1 (15), PKA (47), PKBβ (22), and PKCθ (41), display a very similar overall conformation. As there is much interest in development of specific AGC kinase inhibitors for the treatment of disease, the greater diversity shown between inactive kinase structures indicates that more selective protein kinase inhibitors would be obtained if the inactive forms of kinases were targeted.

Acknowledgments—We thank the European Synchrotron Radiation Facility, Grenoble for the time at beamline ID14-EH1, the Sequencing Service (School of Life Sciences, University of Dundee, Scotland, www.dnaseq.co.uk) for DNA sequencing, Nick Morrice and David Campbell for mass spectroscopy analysis, and the protein production and antibody purification teams (Division of Signal Transduction Therapy, University of Dundee) coordinated by Hilary McLauchlan and James Hastie for expression and purification of PreScission protease.

REFERENCES

1. Mora, A., Komander, D., van Aalten, D. M. F. F., and Alessi, D. R. (2004) *Sem. Cell Dev. Biol.* **15,** 161–170
2. Alessi, D. R., James, S. R., Downes, C. P., Holmes, A. B., Gaffney, P. R., Reese, C. B., and Cohen, P. (1997) *Curr. Biol.* **7,** 261–269
3. Stephens, L., Anderson, K., Stokoe, D., Erdjument-Bromage, H., Painter, G. F., Holmes, A. B., Gaffney, P. R., Reese, C. B., McCormick, F., Tempst, P., Coadwell, J., and Hawkins, P. T. (1998) *Science* **279,** 710–714
4. Balendran, A., Currie, R., Armstrong, C. G., Avruch, J., and Alessi, D. R. (1999) *J. Biol. Chem.* **274,** 37400–37406
5. Komander, D., Fairservice, A., Deak, M., Kular, G. S., Prescott, A. R., Peter Downes, C., Safrany, S. T., Alessi, D. R., and van Aalten, D. M. F. (2004) *EMBO J.* **23,** 3918–3928
6. Brazil, D. P., and Hemmings, B. A. (2001) *Trends Biochem. Sci.* **26,** 657–664
7. Vanhaesebroeck, B., and Alessi, D. R. (2000) *Biochem. J.* **346,** Pt. 3, 561–576
8. Volarevic, S., and Thomas, G. (2001) *Prog. Nucleic Acids Res. Mol. Biol.* **65,** 101–127
9. Lang, F., and Cohen, P. (2001) *Sci. STKE* **2001,** RE17
10. Frodin, M., and Gammeltoft, S. (1999) *Mol. Cell. Endocrinol.* **151,** 65–77
11. Frodin, M., Antal, T. L., Dummler, B. A., Jensen, C. J., Deak, M., Gammeltoft, S., and Biondi, R. M. (2002) *EMBO J.* **21,** 5396–5407
12. Fuse, E., Tanii, H., Takai, K., Asanome, K., Kurata, N., Kobayashi, H., Kuwabara, T., Kobayashi, S., and Sugiyama, Y. (1999) *Cancer Res.* **59,** 1054–1060
13. Biondi, R. M., Cheung, P. C., Casamayor, A., Deak, M., Currie, R. A., and Alessi, D. R. (2000) *EMBO J.* **19,** 979–988
14. Biondi, R. M., Kieloch, A., Currie, R. A., Deak, M., and Alessi, D. R. (2001) *EMBO J.* **20,** 4380–4390
15. Biondi, R. M., Komander, D., Thomas, C. C., Lizcano, J. M., Deak, M., Alessi, D. R., and van Aalten, D. M. F. F. (2002) *EMBO J.* **21,** 4219–4228
16. Casamayor, A., Morrice, N. A., and Alessi, D. R. (1999) *Biochem. J.* **342,** Pt. 2, 287–292
17. Wick, M. J., Ramos, F. J., Chen, H., Quon, M. J., Dong, L. Q., and Liu, F. (2003) *J. Biol. Chem.* **278,** 42913–42919
18. De Bondt, H. L., Rosenblatt, J., Jancarik, J., Jones, H. D., Morgan, D. O., and Kim, S. H. (1993) *Nature* **363,** 595–602
19. Jeffrey, P. D., Russo, A. A., Polyak, K., Gibbs, E., Hurwitz, J., Massague, J., and Pavletich, N. P. (1995) *Nature* **376,** 313–320
20. Russo, A. A., Jeffrey, P. D., and Pavletich, N. P. (1996) *Nat. Struct. Biol.* **3,** 696–700
21. Yang, J., Cron, P., Thompson, V., Good, V. M., Hess, D., Hemmings, B. A., and Barford, D. (2002) *Mol. Cell* **9,** 1227–1240
22. Yang, J., Cron, P., Good, V. M., Thompson, V., Hemmings, B. A., and Barford, D. (2002) *Nat. Struct. Biol.* **9,** 940–944
23. Knighton, D. R., Zheng, J. H., Ten Eyck, L. F., Ashford, V. A., Xuong, N. H., Taylor, S. S., and Sowadski, J. M. (1991) *Science* **253,** 407–414
24. Frodin, M., Jensen, C. J., Merienne, K., and Gammeltoft, S. (2000) *EMBO J.* **19,** 2924–2934
25. Otwinowski, Z., and Minor, W. (1997) *Methods Enzymol.* **276,** 307–326
26. Brunger, A. T., Adams, P. D., Clore, G. M., DeLano, W. L., Gros, P., Grosse-Kunstleve, R. W., Jiang, J. S., Kuszewski, J., Nilges, M., Pannu, N. S., Read, R. J., Rice, L. M., Simonson, T., and Warren, G. L. (1998) *Acta Crystallogr. Sect. D Biol. Crystallogr.* **54,** Pt. 5, 905–921
27. Murshudov, G. N., Vagin, A. A., and Dodson, E. J. (1997) *Acta Crystallogr. Sect. D Biol. Crystallogr.* **53,** 240–255
28. Jones, T. A., Zou, J. Y., Cowan, S. W., and Kjeldgaard, M. (1991) *Acta Crystallogr. Sect. A* **47,** 110–119
29. Schuettelkopf, A. W., and van Aalten, D. M. F. F. (2004) *Acta Crystallogr. Sect. D Biol. Crystallogr.* **60,** 1355–1363
30. Balendran, A., Casamayor, A., Deak, M., Paterson, A., Gaffney, P., Currie, R., Downes, C. P., and Alessi, D. R. (1999) *Curr. Biol.* **9,** 393–404
31. Johnson, L. N., Noble, M. E., and Owen, D. J. (1996) *Cell* **85,** 149–158
32. Nolen, B., Taylor, S., and Ghosh, G. (2004) *Mol. Cell* **15,** 661–675
33. Taylor, S. S., and Radzio-Andzelm, E. (1994) *Structure* **2,** 345–355
34. Leon, B. C., Tsigelny, I., and Adams, J. A. (2001) *Biochemistry* **40,** 10078–10086
35. Gibbs, C. S., and Zoller, M. J. (1991) *J. Biol. Chem.* **266,** 8923–8931
36. Skamnaki, V. T., Owen, D. J., Noble, M. E., Lowe, E. D., Lowe, G., Oikonomakos, N. G., and Johnson, L. N. (1999) *Biochemistry* **38,** 14718–14730
37. George, S., Rochford, J. J., Wolfrum, C., Gray, S. L., Schinner, S., Wilson, J. C., Soos, M. A., Murgatroyd, P. R., Williams, R. M., Acerini, C. L., Dunger, D. B., Barford, D., Umpleby, A. M., Wareham, N. J., Davies, H. A., Schafer, A. J., Stoffel, M., O'Rahilly, S., and Barroso, I. (2004) *Science* **304,** 1325–1328
38. Gibson, R. M., Ji-Buechler, Y., and Taylor, S. S. (1997) *Protein Sci.* **6,** 1825–1834
39. Cox, S., and Taylor, S. S. (1995) *Biochemistry* **34,** 16203–16209
40. Smith, K. J., Carter, P. S., Bridges, A., Horrocks, P., Lewis, C., Pettman, G., Clarke, A., Brown, M., Hughes, J., Wilkinson, M., Bax, B., and Reith, A. (2004) *Structure (Camb.)* **12,** 1067–1077
41. Xu, Z. B., Chaudhary, D., Olland, S., Wolfrom, S., Czerwinski, R., Malakian, K., Lin, L., Stahl, M. L., Joseph-McCarthy, D., Benander, C., Fitz, L., Greco, R., Somers, W. S., and Mosyak, L. (2004) *J. Biol. Chem.* **279,** 50401–50409
42. Dajani, R., Fraser, E., Roe, S. M., Young, N., Good, V., Dale, T. C., and Pearl, L. H. (2001) *Cell* **105,** 721–732
43. ter Haar, E., Coll, J. T., Austen, D. A., Hsiao, H. M., Swenson, L., and Jain, J. (2001) *Nat. Struct. Biol.* **8,** 593–596
44. Chen, P., Luo, C., Deng, Y., Ryan, K., Register, J., Margosiak, S., Tempczyk-Russell, A., Nguyen, B., Myers, P., Lundgren, K., Kan, C. C., and O'Connor, P. M. (2000) *Cell* **100,** 681–692
45. Longenecker, K. L., Roach, P. J., and Hurley, T. D. (1996) *J. Mol. Biol.* **257,** 618–631
46. Lowe, E. D., Noble, M. E., Skamnaki, V. T., Oikonomakos, N. G., Owen, D. J., and Johnson, L. N. (1997) *EMBO J.* **16,** 6646–6658
47. Yang, J., Ten Eyck, L. F., Xuong, N. H., and Taylor, S. S. (2004) *J. Mol. Biol.* **336,** 473–487